The structure and dynamics of CO_2 on NaCl(001) studied by helium atom scattering

G. Lange, D. Schmicker, J. P. Toennies, R. Vollmer, and H. Weiss[a)]
Max-Planck-Institut für Strömungsforschung, Bunsenstr. 10, 37073 Göttingen, Germany

(Received 30 January 1995; accepted 2 May 1995)

The structure and dynamics of physisorbed carbon dioxide on *in situ* cleaved single crystal sodium chloride surfaces was studied by means of elastic as well as inelastic helium atom scattering. At $T_{\text{surface}}=80-83.5$ K the diffraction patterns indicate a commensurate (2×1) monolayer superstructure on the (001) plane of the substrate, the unit cell containing a glide plane. This is in agreement with results obtained from low energy electron diffraction and infrared spectroscopy. In time-of-flight experiments single phonon low-energy loss and gain features were observed which can be attributed to acoustic and optical modes. Two higher-energy features are probably due to the first combination modes observed by helium atom scattering so far. The growth of solid CO_2 adsorbed on NaCl(001) was also studied. © *1995 American Institute of Physics.*

I. INTRODUCTION

The physisorption of small molecules on alkali halide single crystal surfaces is of interest from both the experimental[1–18] and the theoretical point of view.[19–26] The interactions between adsorbate and substrate are of electrostatic and van der Waals nature, involving essentially additive two-body interactions.[27] Since these interactions are better understood than the interactions in analogous metal systems the alkali halides are ideal substrates for studying the structure and dynamics of the adsorbates and their phase transitions. However, the sensitivity of alkali halides to electron beams has so far hampered the experimental investigation of adsorbates on these surfaces. Only recently Schimmelpfennig *et al.* reported for the first time a LEED study of CO_2 adsorbed on epitaxially grown, high-quality thin NaCl(001) films on a Ge(001) substrate.[16] Most of our present knowledge on the physisorption on well-defined alkali halide single crystal surfaces originates from Fourier-transform infrared (FTIR) spectroscopy. Particularly the adsorption of CO and CO_2 on NaCl(001) was extensively studied by Ewing and co-workers[1,10–12] and Heidberg and co-workers.[2–8,20,21] Although it was possible to draw some conclusions about the adsorbate structure, infrared spectroscopy does not provide direct information on the symmetry of the adsorbate lattice. In helium atom scattering (HAS) nearly monoenergetic helium atoms with kinetic energies between typically 10–80 meV are scattered from the surface. The angular distributions provide diffraction information on the surface lattice structure, while the time-of-flight (TOF) spectra provide information on the frequencies of the low-energy vibrational modes. Since helium atoms are neutral there are no surface charging problems as in LEED, and at the low beam energies the method is definitely nondestructive. We have already shown that HAS is a valuable tool for studies of adsorption on alkali halide single crystal surfaces. A two-dimensional phase transition in the monolayer CO/NaCl(001) was reported and, in conjunction with infrared spectroscopy, characterized for the first time.[2,14] In a previous brief communication on CO_2/NaCl(001) HAS has been shown to be well-suited to determine the low-energy vibrational motions of adsorbates on alkali halides.[7,15] In the present study the 2D lattice structure of monolayer and multilayer CO_2 on NaCl(001) was investigated by HAS. The previously reported TOF studies were extended to the energy range 10–30 meV and these results are also presented here.

Our present knowledge on the structure of the monolayer adsorbate CO_2/NaCl(001) is mainly based on infrared (IR) studies in which the existence of a two-dimensional first-order phase transition with increasing coverage was established.[3,5,8] Below the 2D transition pressure p_T^{2D}, corresponding to coverages below about 2% of a full monolayer, a 2D lattice gas is formed, with molecules oriented parallel to the surface. At p_T^{2D} large islands with monolayer structure coexist with the 2D gas, while above p_T^{2D} the full monolayer is thermodynamically stable. From the infrared spectra it was concluded that in the monolayer the molecules are adsorbed in a herringbonelike arrangement, with at least two molecules per unit cell which are tilted by about 27° relative to the surface plane.[5,10] In the LEED study by Schimmelpfennig *et al.* a (2×1) superstructure was reported for the monolayer CO_2/NaCl(001).[16] Two CO_2 molecules in each unit cell are mapped on each other by a glide plane. Based on this (2×1) superstructure, a more accurate simulation of the measured infrared spectra yields a tilt angle ϑ of ~34° and an intermolecular azimuthal angle φ of ~80°,[6] in good agreement to $T=0$ K potential energy calculations ($\vartheta=26°$, $\varphi=86°$).[20,21] These results are somewhat different to those obtained by Liu *et al.*[17] On the basis of helium diffraction experiments these authors report a (2×1) structure for submonolayer coverages only, while for the monolayer a $(2\sqrt{2}\times2\sqrt{2})R45°$ unit mesh is suggested, the unit cell of the latter structure containing eight CO_2 molecules. One of the goals of the present study was to clarify this structural uncertainty.

The vibrational normal mode frequencies of a CO_2 molecule in a (2×1) CO_2 monolayer adsorbate on a rigid NaCl(001) surface have already been predicted theoretically

[a)]Permanent address: Institut für Physikalische Chemie und Elektrochemie, Universität Hannover, Callinstr, 3-3a, 30173 Hannover, Germany.

at the zone origin $\bar{\Gamma}$ for the in-phase vibration.[20,21] The results indicate five different normal modes for the vibrational motions of the molecules with respect to the surface which all lie in the energy range from about 17 to 71 cm^{-1}, corresponding to 2.2 to 8.9 meV. The accurate knowledge of these vibrational modes is of importance for understanding and modeling the adsorbate-substrate potential which governs processes like diffusion, desorption, and vibrational line-broadening mechanisms (dephasing). The energies of these modes are too low to be presently measured by e.g. infrared spectroscopy and are only accessible to HAS.

This paper starts with a brief description of the apparatus and the experimental conditions. The HAS data for the structures of the CO_2 monolayer as well as the CO_2 solid are presented in Sec. III. We will also present data on the frequencies and phonon dispersion curves of CO_2 molecules vibrating relative to the NaCl surface obtained by inelastic time-of-flight scattering experiments. In Sec. IV the adsorbate lattice structure is discussed and compared to previous LEED (Ref. 16) and helium diffraction studies.[17] The measured CO_2/NaCl(001) vibrations are discussed on the basis of the calculated normal modes,[20,21] and a recent theoretical study of the CO_2 phonons.[26] A summary and conclusions follow in Sec. V.

II. EXPERIMENT

A highly monoenergetic He beam with a velocity spread of $\Delta v/v \approx 0.5\%$ is produced by a supersonic expansion from a high pressure (10–400 bar) into vacuum, through a small hole of 10 μm in diameter. After scattering from the sample the He atoms are detected by a magnetic mass spectrometer mounted at the end of a 1.428 m long flight tube. The angle between incident and scattered beam is fixed at $\theta_{SD}=90°$. The scattering plane contains the surface normal in all measurements. Different momentum transfers $\Delta K_{\parallel}$ parallel to the surface are probed by rotating the sample around an axis perpendicular to the sagittal plane (polar rotation). The polar angle of incidence θ_i onto the sample is measured with respect to the surface normal. Thus the elastic scattering is simply given by $\Delta K_{\parallel}=k_i(\sin\theta_f-\sin\theta_i)$, where $\theta_f=\theta_{SD}-\theta_i$. For time-of-flight measurements the helium beam can be chopped with a variable-speed, variable-pulse-width chopper. For more details the reader is referred to Refs. 28 and 29.

Most of the diffraction and TOF experiments were carried out with $E_i=14$ meV incident beam energy, corresponding to an incident wave vector $k_i=5.17$ Å^{-1}. The overall energy resolution was $\sim$0.35 meV for this k_i. In order to excite higher-energy modes and to scan across a larger range in reciprocal space angular distributions as well as TOF experiments were also measured at $E_i=33.5$ meV ($k_i=8.02$ Å^{-1}).

Two different NaCl single crystals of about $6\times6\times8$ mm^3 size, purchased from Korth,[30] were used. They were mounted on a *xyz* manipulator with provisions for sample tilt as well as azimuthal and polar rotation. The surfaces used for the scattering experiments were prepared by *in situ* cleavage under ultrahigh vacuum conditions after bakeout of the chamber (base pressure $<1\times10^{-10}$ mbar). A NiCr/Ni thermocouple was attached to the crystal by inserting it into a hole drilled into one side and plugging the hole up with NaCl powder. The thermocouple was calibrated against liquid nitrogen and room temperature. Temperatures below 30 K were obtainable by liquid He cooling. Temperatures above this lower limit could be adjusted with better than ±0.1 K stability by a computer-regulated heater embedded in the sample holder. Although the relative accuracy and reproducibility of the sample temperature is better than 0.5 K, we do not regard the absolute accuracy as better than 2 K. In order to avoid contamination and to clean the surface from adsorbates the sample was heated to 350 K between scattering experiments. The low defect concentration and surface cleanliness were confirmed by the reproducible observation of weak features in addition to the sharp and intense diffraction peaks, the intensities of these features being about two orders of magnitude smaller than that of the specular peak. These features are attributed to single phonon inelastic processes, which are either resonantly enhanced by selective adsorption or by a special kinematical effect called kinematical focusing.[28,31,32] They are very sensitive to surface defects and indicate a clean, high-quality surface.

Carbon dioxide (purity >99.995%, Messer Griesheim) was admitted into the target chamber via a leak valve. The monolayer was prepared by exposing the sample to 2×10^{-8} mbar of CO_2 at sample temperatures $T_s=80$ and 83.5 K, respectively. It is important to note that the presented data were collected under equilibrium conditions comparable to those of the infrared experiments. Extensive IR studies showed that under these conditions sharp spectral features indicative of a well-ordered structure can be observed.[3] In particular, the integrated IR absorption of these features was found to be independent of pressure over more than two orders-of-magnitude. At higher pressures the spectral features of three-dimensional solid appear. From this it was concluded that the observed absorptions are due to a monolayer. In the present study, the surface coverage was monitored by following the intensity of the specularly reflected helium atom beam during exposure.[33] A typical plot of the specular intensity as a function of CO_2 coverage and sample temperature is shown in Fig. 1 for the $\langle110\rangle$ azimuthal direction. After the CO_2 pressure was set to 2×10^{-8} mbar at $T_s=80$ K (a) the intensity first dropped off rapidly by about 15% in an exponential decay. Subsequently the specular intensity fell significantly slower down to a constant value of about 4×10^5 counts per second (cps) at which point gas admission could be stopped (b). The observed loss in specular intensity of the CO_2 layer as compared to the bare NaCl surface is attributed mainly to the greater Debye–Waller attenuation of the adsorbate layer. The somewhat steeper decrease below a beam intensity of $\sim10^6$ cps is due to partial saturation of the detector above this atom count rate. The specular intensity at (b) remained the same even after the CO_2 pressure had been reduced to $\leqslant1\times10^{-10}$ mbar (at $T_s=83.5$ K slow desorption occured when the CO_2 partial pressure was lowered to $<1\times10^{-10}$ mbar, in agreement with results from the IR experiments. In this case a CO_2 pressure of 1×10^{-9} mbar was sufficient to keep the coverage constant). Since the coverage did not change in the pressure range of $p(CO_2)$

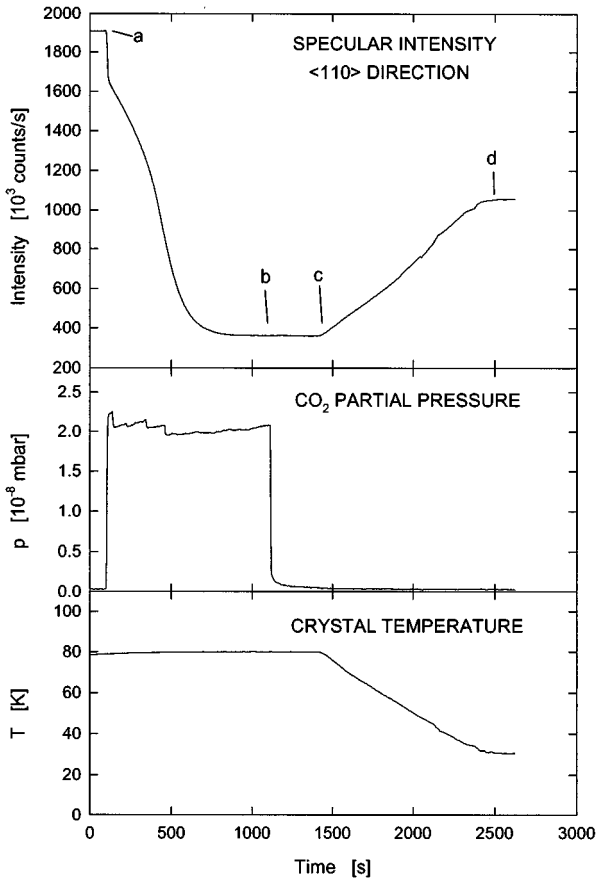

FIG. 1. Specular intensity of the He atom beam, CO_2 pressure, and crystal temperature during exposure of the sample to CO_2. $T_s=80$ K, ⟨110⟩ direction. (a) $p(CO_2)$ adjusted to 2×10^{-8} mbar. (b) Flow of CO_2 stopped. (c) Cooling from 80 K to 30 K. (d) $k_i=5.17$ Å^{-1}.

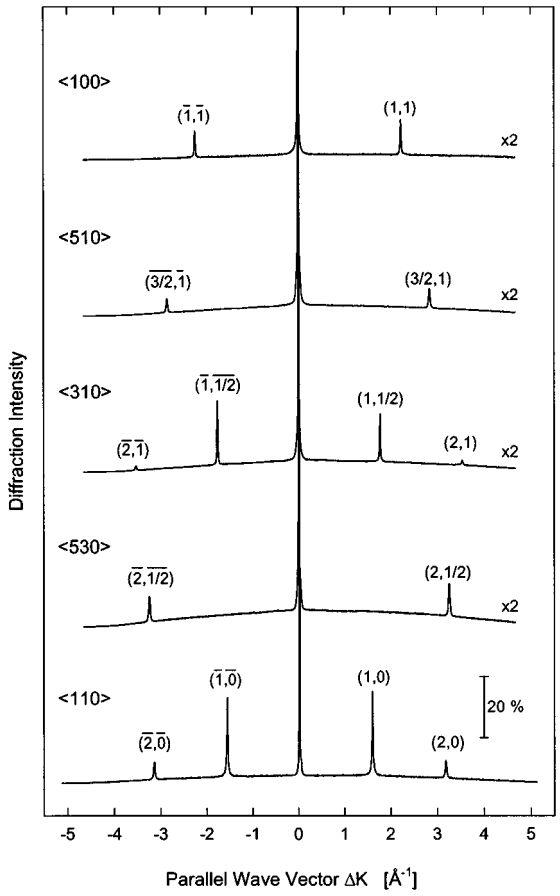

FIG. 2. Measured diffraction patterns of monolayer CO_2 on NaCl(001) for different azimuthal directions. $T_s=83.5$ K. $p(CO_2)=1\times10^{-9}$ mbar. $k_i=5.17$ Å^{-1}. The specular intensities are normalized to 1. Azimuthal directions are referenced to the NaCl(001) substrate lattice (compare Fig. 3).

$=1\times10^{-9}$–2×10^{-8} mbar at $T_s=80-83.5$ K we infer that near-equilibrium conditions were achieved, and that the monolayer coverage was established. The adsorbate lattice structure reported below was measured under these conditions.

Due to the high resolution of the HAS apparatus an azimuthal accuracy of better than ~0.1° is necessary to scan a certain azimuth. This accuracy was achieved by first adjusting the bare NaCl crystal until the diffraction pattern expected for a certain azimuth was obtained and then dosing with CO_2 using the procedure described above. In experiments in which solid CO_2 was grown on top of the monolayer at $T_s=55$ K, a low deposition rate between 0.01 and 0.1 L s^{-1} was chosen in order to prepare multilayers as well-ordered as possible (1 L≡1 langmuir≡10^{-6} Torr s). For the TOF experiments the monolayer was prepared at $T_s=80$ K, as described above. Then the gas flow was stopped and the sample cooled down from 80 K [Fig. 1(c)] to 30 K [Fig. 1(d)] in order to suppress the multiphonon background in the TOF spectra. The observed increase in scattering intensity by a factor of 3–4 is attributed to a decrease of the Debye–Waller attenuation. An increase in coverage on the other hand, if present, would have led to a decrease in intensity, as was observed upon growth of multilayers on top of the monolayer. After every three to six TOF spectra the monolayer was desorbed by heating the sample to above 170 K and a new monolayer was then prepared using the procedure described above. TOF spectra at the end of a measuring period agreed with those taken immediately after preparation so that effects due to contamination could be ruled out.

III. RESULTS

Angular distributions of the total (elastically and inelastically) scattered intensity were measured under adsorption–desorption equilibrium conditions for a total of five different azimuthal directions, providing diffraction patterns of a CO_2 monolayer on NaCl(001). In Fig. 2 the results are presented as a function of parallel momentum transfer $\Delta K_\parallel = k_i(\sin\theta_f - \sin\theta_i)$ for an incident wave vector $k_i=5.17$ Å^{-1} of the helium atom beam. The angular distributions show the expected symmetry with respect to the specular peak at the origin. All diffraction peaks observed for the adsorbate have reciprocal lattice vectors which correspond to substrate reciprocal lattice vectors or to half of such a vector which indicates that the adsorbate forms a structure commensurate to the underlying NaCl lattice. For this reason peaks are labeled according to the NaCl reciprocal lattice shown in Fig. 3(a). Furthermore the peak width is the same as for the clean surface. Thus all the evidence is that a very

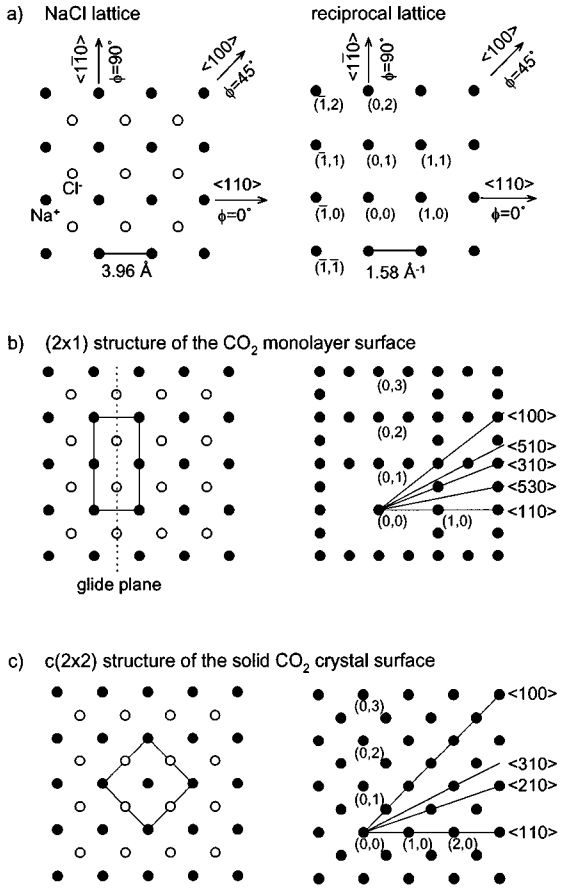

FIG. 3. (a) Real and reciprocal lattice of clean NaCl. (b) Real and reciprocal lattice of the (2×1) superstructure of a monolayer of CO_2, measured at $T_s=83.5$ K. Four domains are rotated by 90° to each other. Half-order diffraction peaks are missing in the $\langle 110\rangle$ and $\langle 1\bar{1}0\rangle$ direction, indicating the glide plane which is marked by the dashed line in the real space drawing. (c) Real and reciprocal lattice of the $c(2\times2)$ superstructure of a CO_2 crystal surface, measured at $T_s=55$ K.

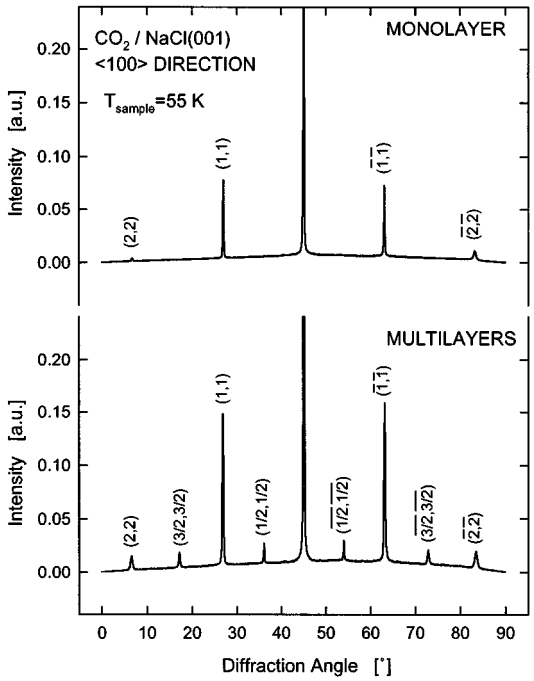

FIG. 4. Measured diffraction patterns of CO_2 on NaCl(001), $\langle 100\rangle$ direction. Top, monolayer CO_2/NaCl(001). Bottom, multilayers CO_2 formed after exposure to ~170 L. $T_s=55$ K.

well-ordered, defect-free adsorbate layer is formed, with domain sizes in excess of the transfer width of the apparatus, which is about 450 Å.[34]

The additional half-order diffraction peaks observed in some of the azimuthal scans indicate the formation of a superstructure. The reciprocal lattice shown in Fig. 3(b) is in agreement with all measured diffraction spots. It corresponds to a (2×1) superstructure, which—due to the C_{4v} symmetry of the NaCl surface—exists in domains rotated by 90° to each other. It should be noted that the (2×1) structure is the only superlattice which can explain all observed diffraction peaks. All other, higher-index superstructures would exhibit additional diffraction peaks along the scanned azimuthal directions and can therefore be excluded. It is also important to note that the half-order peaks expected for a (2×1) structure are missing in the $\langle 110\rangle$ direction ($\phi=0°$). This is indicative of glide symmetry lines along this direction of the adsorbate lattice and also, due to the existence of different domains, along the $\langle 1\bar{1}0\rangle$ direction.[35] The glide plane which is marked in Fig. 3(b) by a dashed line restricts the space group of the (2×1) adsorbate lattice structure to pg symmetry.[36] As another check on the assumed structure some angular distributions were measured over a larger portion of the reciprocal space at an incident wave vector $k_i=8.02$ Å^{-1}. No additional diffraction peaks not in agreement with the (2×1) superlattice and the glide plane structure were found.

Upon formation of the three-dimensional CO_2 solid on top of the monolayer at $T_s=55$ K the most prominent changes in the diffraction pattern are observed in the $\langle 100\rangle$ direction ($\phi=45°$). Now additional half-order peaks not found for the monolayer are detected (Fig. 4). All the diffraction spots observed at ~170 L can be accounted for by assuming a $c(2\times2)$ multilayer structure. The corresponding pattern in reciprocal space is shown in Fig. 3(c). Up to an exposure of ~170 L the diffraction intensity of all peaks measured along the $\langle 100\rangle$ direction increases relative to that of the specular peak. However, the absolute intensity of the specular and other diffraction peaks decreases while the background increases. At the same time, the $(1,\frac{1}{2})$ superstructure peak as well as other peaks characteristic for the (2×1) monolayer structure decrease slowly in intensity and almost disappear for an exposure of ~170 L. As a consequence in the exposure range between that corresponding to a full monolayer and ~170 L the diffraction pattern is a superposition of the (2×1) and the $c(2\times2)$ patterns, resulting in an apparent $p(2\times2)$ pattern. No additional peaks not in agreement with these symmetries or their superposition were observed. Finally we note that the diffraction peaks observed for solid CO_2 are somewhat broader than those observed for the clean NaCl(001) surface and for the monolayer CO_2. The additional width indicates the presence of domains or distinct crystallite faces with a size of about 250 Å. From the spacing of the diffraction peaks which agrees within the instrumental resolution with that of the NaCl lattice it appears that the

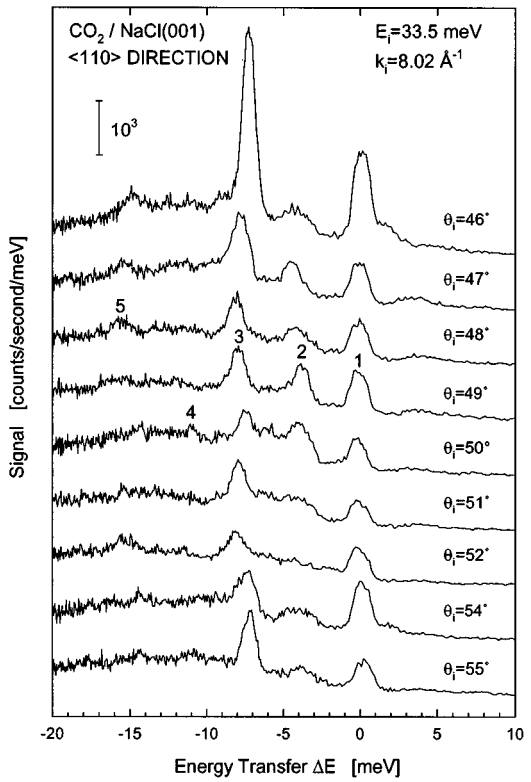

FIG. 5. Time-of-flight distributions of He atoms scattered from a monolayer CO_2, measured along the ⟨110⟩ direction for different angles of incidence θ_i. $T_s=30$ K. $E_i=33.5$ meV, $k_i=8.02$ Å^{-1}. 3×10^5 TOF measurements accumulated.

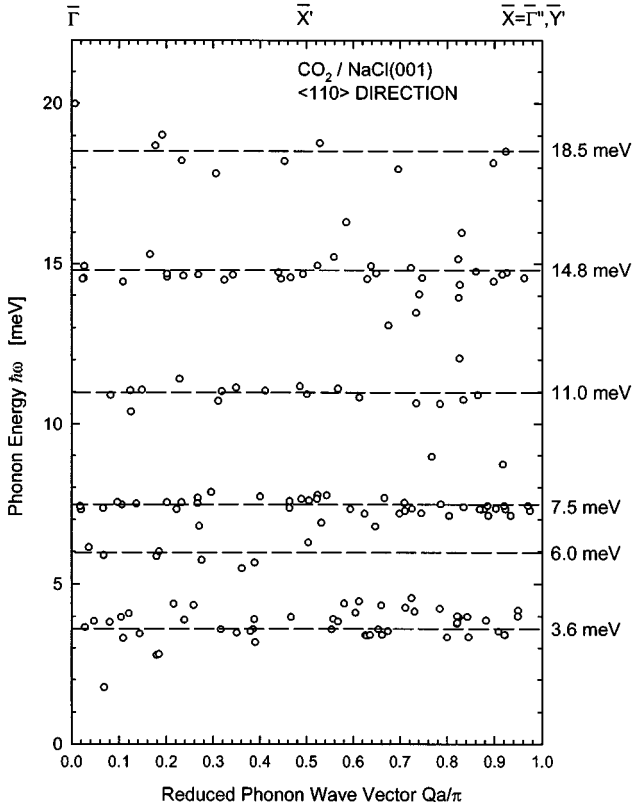

FIG. 6. Phonon dispersion curves for monolayer CO_2 on NaCl. Data were measured along the ⟨110⟩ direction. $T_s=30$ K. $E_i=33.5$ meV, $k_i=8.02$ Å^{-1}.

multilayer adsorbate structure is commensurate. This is consistent with the almost perfect match of the lattice constants of solid CO_2 and NaCl (see below).

Next we present the time-of-flight (TOF) measurements obtained for the monolayer CO_2/NaCl(001). In Fig. 5 a representative series of TOF spectra converted to the energy transfer scale is shown for an incident beam energy $E_i=33.5$ meV (incident wave vector $k_i=8.02$ Å^{-1}) and the azimuthal direction ⟨110⟩. The broad underlying peak below the elastic and phonon peaks is caused by inelastic scattering from defects as well as by multiphonon scattering. In order to minimize the latter contribution the TOF measurements were carried out at the lowest possible temperature of $T_s=30$ K. On top of the broad background several sharp peaks are seen. One of them, labeled peak 1, coincides with the elastic intensity measured at diffraction angles corresponding to reciprocal lattice points and is therefore assigned to elastic scattering from defects. All other peaks correspond to inelastic processes. We attribute the peaks labeled 2 and 3 to one-phonon creation events. There are further, although much weaker peaks (4,5) at even larger flight times which, as will be discussed below, we attribute to overtone and combination excitation.

For the 90° fixed-angle geometry between incoming and outgoing beam the parallel momentum transfer ΔK parallel to the surface corresponding to the energy loss or gain ΔE of each of the inelastic peaks is given by the so-called ''scan curve''

$$\frac{\Delta E}{E_i}=\frac{(\sin\theta_i+\Delta K/k_i)^2}{\cos^2\theta_i}-1, \tag{1}$$

where θ_i is the angle of incidence with respect to the surface normal, E_i is the energy of the incident beam, and k_i its wave vector.[28] Thus from a series of TOF spectra measured at different incident angles θ_i many points in the $\Delta K,\Delta E$ plane are determined. In presenting the data from all the TOF spectra measured for the incident beam energy $E_i=33.5$ meV and $29°\leqslant\theta_i\leqslant53°$ some of which are shown in Fig. 5 it is customary to transform the parallel momentum transfer into the first Brillouin zone of the NaCl(001) surface lattice by subtracting the corresponding reciprocal lattice vector G: $Q=\Delta K-G$, and to display only the absolute value of energy and wave vector. As can be seen from Fig. 6, several modes can be distinguished, the mean energies being 3.6 ± 0.2, 6.0 ± 0.2, 7.5 ± 0.2, 11.0 ± 0.2, 14.8 ± 0.2, and 18.5 ± 0.2 meV, respectively. The scatter in the data points suggests some degree of dispersion or a superposition of modes, which are not resolved under the given total experimental resolution of ~1 meV at $E_i=33.5$ meV. Since the higher-lying modes are multiples of the lower-lying ones, they could be due to two- or three-phonon processes, and only the curves at 3.6 meV, 6.0 meV, and 7.5 meV can be assigned with confidence to one-phonon dispersion curves. Within the error limits, the 11 meV loss can be considered as a combination of a 3.6 and a 7.5 meV phonon, the 14.8 meV loss as due to two 7.5 meV phonons, and the 18.5 meV curve as a three-phonon process

involving two 7.5 meV and one 3.6 meV phonons. The 7.5 meV feature cannot be attributed to a two 3.6 meV phonon process since its intensity is always larger than that of the 3.6 meV loss, while the peaks attributed to multiphonon processes are expected to have much smaller intensities. The labels X and X' in Fig. 6 refer to different reciprocal lattice points and different domain orientations as will be explained in more detail below.

In order to investigate these structures in more detail TOF measurements were performed at a lower incident beam energy $E_i=14$ meV ($k_i=5.17$ Å^{-1}), at $T_s=30$ K. At this lower wave vector the contribution of multiphonon scattering is greatly reduced and the energy resolution of the apparatus is more than a factor of 2 greater than at $E_i=33.5$ meV. A representative series of TOF measurements converted to an energy transfer scale is shown in Fig. 7. As compared to the 33.5 meV measurements, many more modes are resolved in the low-energy range below 10 meV. In Fig. 8 the corresponding phonon energy vs phonon wave vector diagram is plotted. The lines through the data points are intended as guides for the eye. This assignment is by no means unique and must be regarded as preliminary. As will be discussed in more detail in Sec. IV, mode crossings are not expected for modes of the same symmetry and suggest that the modes correspond to different directions or different symmetries, labeled with a and b, respectively. Within a set of branches the modes were numbered with increasing energy at the zone boundary.

The dashed curve in Fig. 8 corresponds to the Rayleigh mode of the bare NaCl(001) surface. It is known from previous HAS experiments[37] and was also reproduced in our measurements. This mode generally lies slightly below the projected band of transverse polarized bulk modes as indicated in Fig. 8. Adsorbate modes to the right (greater Q) or below this band can only couple to the bulk when they cross the Rayleigh mode, and are therefore mainly located in the topmost layer in the CO_2 adlayer. In the bulk band region the vibrational modes of the CO_2 layer can mix with the bulk bands and become a resonance.[33,38] If the coupling is very strong their amplitude at the surface may be reduced to such an extent that they are no longer observed in the experiment. The latter appears to be the case for the adsorbate modes with frequencies less than about 6 meV. Apparently the density of surface projected bulk phonons is so high that the coupling is sufficiently strong to completely suppress the surface vibrations.

Starting from the highest energy we identify a new mode (VI) at about 9 meV which we attribute to an optical mode. The 7.5 meV mode which was already observed in the $E_i=33.5$ meV experiments is clearly seen also at small wave vectors. Surprisingly it appears to disappear beyond the bulk band edge. Very likely it hybridizes with the Rayleigh mode as frequently observed in other systems (see e.g., Refs. 33 and 38). If this is the case than the mode IIIb is its continuation in the region where a coupling with the substrate is not allowed. The mode IIIa shows a nice dispersion with a minimum at X' and can very likely be assigned to a collective transverse vibrational motion with a distinct coupling between the CO_2 molecules. The three modes I, IIa, and IIb

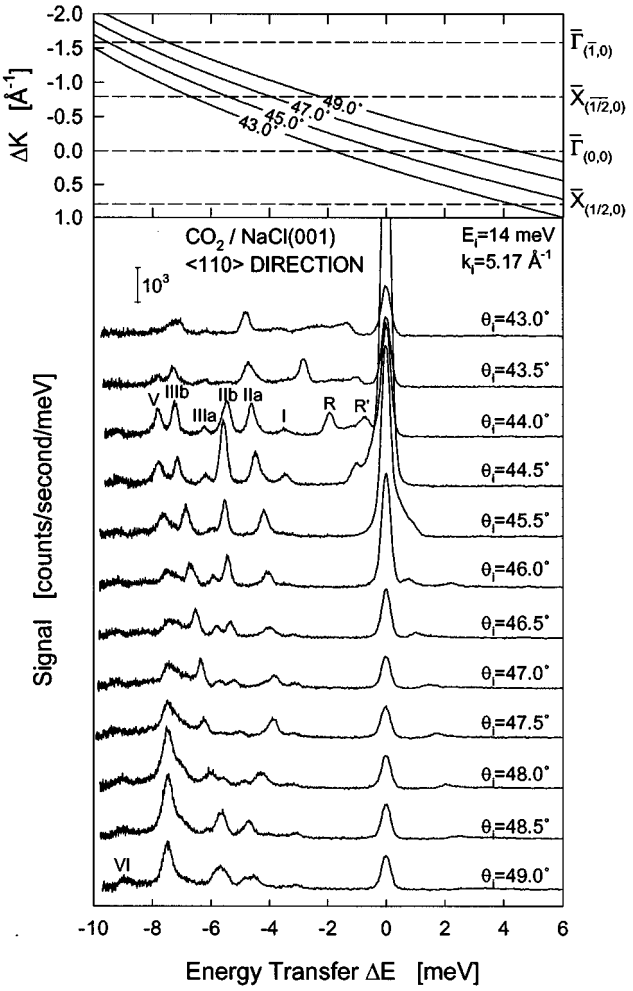

FIG. 7. A series of time-of-flight distributions of He atoms scattered from a monolayer CO_2, measured along the $\langle 110\rangle$ direction for varying angles of incidence θ_i. $T_s=30$ K. $E_i=14$ meV, $k_i=5.17$ Å^{-1}. 1.5×10^6 TOF measurements accumulated, except for $\theta_i=45°$, where 3×10^5 measurements were accumulated. TOF spectra at the end of a typical measuring period of 6 h agreed with those taken immediately after preparation so that any effect of contamination could be ruled out. The peak at $\Delta E=0$ is attributed to elastic scattering from random defects, the other peaks are due to single phonon creation or annihilation. The phonon labels exemplary shown for the 44.0° spectrum are explained in the text. The TOF spectrum at $\theta_i=45°$ is not presented since it shows mainly the very intense specular peak. The parallel momentum transfers of the phonon peaks in the TOF spectra are identified via the scan curves shown at the top for selected angles. Features due to the Rayleigh phonon are denoted R and R', respectively.

below mode IIIa may also show dispersion but because of the strong coupling with the bulk bands they cannot be observed at small wave vectors. The modes V and VI are very pronounced at the zone origin $\bar{\Gamma}$. At X' the mode IIa has the highest intensity and modes IIIb, IV, and V are clearly visible while all other modes are weak. At $Q=\pi/a$ six modes were observed from which modes IIb, IIIb, and VI are strongest.

Only a few time-of-flight spectra were measured at $T_s=83.5$ K. The observed energy loss and gain features were in agreement with those shown above. Thus we can conclude that the results are due to a monolayer and not a multilayer of CO_2. Moreover, diffraction patterns measured

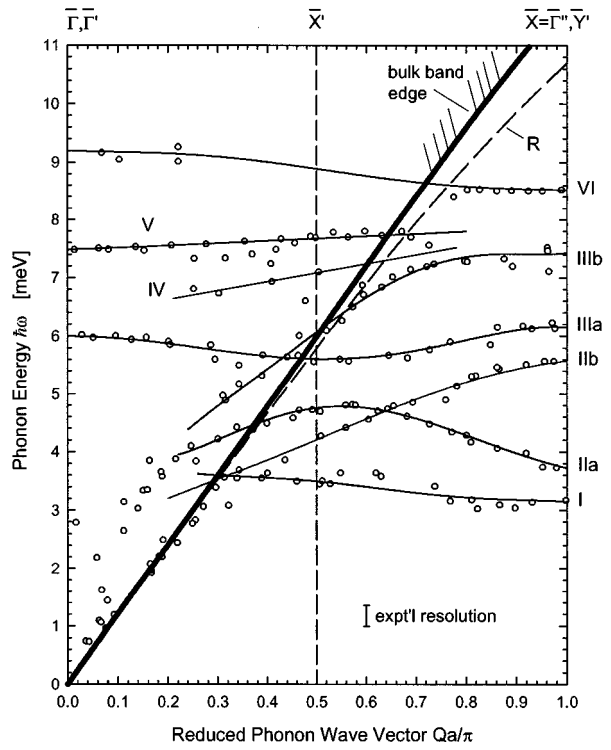

FIG. 8. Measured phonon dispersion curves of the monolayer CO_2/NaCl(001) along the ⟨110⟩ azimuthal direction, with $a=3.96$ Å. $E_i=14$ meV. The phonon branch labeling is explained in the text. The Rayleigh mode R and the bulk phonon edge are adapted from Ref. 37.

at 30 K prior to the inelastic scattering experiments (after cooling down from 80 K) were in agreement with the existence of only the (2×1) monolayer structure described above.

IV. DISCUSSION

Our results for the monolayer structure of CO_2 on NaCl(001) single crystal surfaces at $T_s=83.5$ K indicate the formation of a (2×1) unit cell, which is of pg symmetry and contains a glide plane. This observation is in agreement with results from Fourier-transform infrared spectroscopy[3,5,6,8,10,11,20] as well as with LEED data.[16] In infrared spectroscopy a correlation field splitting of internal CO_2 vibrations was observed and attributed to at least two molecules per unit cell. By means of isotope mixture experiments Heidberg *et al.* could prove that these molecules occupy identical adsorption sites, a prerequisite for the glide plane observed in this study.[3,5] From a plane group symmetry analysis Berg and Ewing suggested that the (2×1) structure can be explained by arranging two tilted molecules in each surface unit cell in a herringbonelike fashion.[10] This arrangement was confirmed by extended spectra simulations as well as theoretical modeling.[5,6,20,21,25]

Schimmelpfennig *et al.* have published low-energy electron diffraction (LEED) data for the same system.[16] In these experiments NaCl films of a few nm thickness epitaxially grown on Ge(001) were used as substrates. HAS diffraction experiments on NaCl films prepared in the same way indicate that these surfaces are of almost the same quality as the cleaved ones used here.[39] In agreement with our results the CO_2/NaCl monolayer LEED diffraction pattern corresponds to a (2×1) structure, the unit cell containing a glide plane. This result is further confirmed by LEED measurements on CO_2 adsorbed on cleaved NaCl(001) single crystal planes, which became possible by using a very low primary beam current and a channeltron detection system.[40] In the LEED experiments as well as in the present study the width of the diffraction peaks is limited by the instrumental resolution, suggesting domain sizes in excess of 450 Å.

In the FTIR studies a first-order phase transition between a two-dimensional CO_2 lattice gas and a two-dimensional condensed phase, i.e., the monolayer, was observed.[3,5] On the highest-quality NaCl single crystal surfaces the maximum density of the 2D gas was found to be $<2\%$ of the monolayer density. For a given temperature, coexistence of the two phases is possible only at a transition pressure p_T^{2D}. At this pressure, the observed absorption frequencies made it possible to distinguish unambiguously between the 2D gas and the 2D condensed phase. The vibrational frequencies and the linewidth of the 2D condensed phase were found to be insensitive to surface coverage, again indicating growth of fairly large islands.

The growth mechanism of the monolayer, observed in this HAS study, is in agreement with these infrared and the LEED data. Because of the exceptional sensitivity of HAS to surface defects[41,42] the specularly reflected helium atom beam intensity usually shows a sharp maximum at completion of a monolayer and passes through a minimum in between. With increasing exposure the adlayer on the originally well-ordered surface will have an increasing density of defects and high concentration of step edges which is largest when half a monolayer is deposited. With further adsorption a well-ordered first monolayer adsorbate surface is produced. This behavior, which has been frequently observed, for example in the epitaxial growth of Cu on Cu(100),[43] NaCl on Ge(001),[39] and for the growth of the monolayer CO on NaCl(001),[44] was not observed in the present case. Under the equilibrium conditions the intensity of the specularly reflected helium beam was found to decrease continuously until finally the monolayer coverage is established (see Fig. 1). Apparently in this system growth proceeds by the formation of a small number of large two-dimensional islands, and therefore a small number of ''surface defects'' like steps and isolated molecules. This can also be inferred from the width of diffraction peaks measured for submonolayers CO_2 on NaCl(001). The widths were comparable to those of bare NaCl(001) and to the full monolayer, again limited by the instrumental resolution. This indicates the existence of large islands with a lower limit of $\sim$450 Å in diameter, corresponding to more than 10^4 molecules and even larger than the lower limit of 200 Å observed in the LEED experiments.

Under the given conditions of adsorbate preparation the 2D gas phase manifests itself in this HAS study by the very steep decrease of the specular intensity immediately after the first exposure of the clean NaCl(001) surface to CO_2 (see Fig. 1). The steepness suggests a rapidly increasing number of ''defects,'' i.e., isolated CO_2 molecules. Upon growth of 2D islands the decrease in intensity with increasing CO_2 coverage becomes smaller and is mainly due to the altered

Debye–Waller attenuation of the CO_2 layer as compared to the bare NaCl(100) surface.

The observed epitaxial growth and the $c(2\times2)$ symmetry of thicker CO_2 layers grown on top of the monolayer CO_2/NaCl(001) are readily understandable. Crystalline carbon dioxide has a cubic structure which to within 1% has the same lattice constant as bulk NaCl ($a_{\mathrm{NaCl,bulk}}=5.6$ Å at 100 K),[45] allowing almost perfect lattice matching when the CO_2(001) plane is in registry with the NaCl(001) plane [see also Fig. 3(c)]. Somewhat surprising is the slow appearance of this $c(2\times2)$ structure and, simultaneously, the slow disappearance of the (2×1) monolayer structure. Due to the superposition of both structures a $p(2\times2)$ symmetry is observed for a certain range of exposures. There are three possible reasons for this superposition. (i) The sticking coefficient at $T_s=55-65$ K is much smaller than unity, and up to an exposure of ~170 L we observe scattering from very few layers of solid CO_2 which coexist with the monolayer. (ii) Solid CO_2 shows cluster or pyramidal growth instead of layer-by-layer growth, i.e., the growth mechanism is of the Stranski–Krastanov rather than of the Frank–van der Merwe-type.[46] In this case also, and for low enough exposures, multilayers of CO_2 coexist with monolayer regions. (iii) The monolayer imposes its structure onto the first few layers of the solid grown on-top of the monolayer. In the LEED study of Schimmelpfennig *et al.* a coexistence range of the (2×1) and the $c(2\times2)$ structures was also observed at sample temperatures of about 80 K.[16] These authors found evidence for facet spots in the $\langle110\rangle$ direction indicating (111)-facets of CO_2 pyramids. In the present study we found no diffraction spots which would indicate pyramidal growth. However, as mentioned above, the pronounced decrease of scattering intensity with exposure and the somewhat broadened diffraction peaks suggest the formation of small but crystalline CO_2 clusters. More studies involving varying preparation and annealing conditions are necessary in order to answer the question which of the proposed mechanisms contribute to the intermediately observed $p(2\times2)$ structure.

Having discussed the structures of monolayer as well as multilayer CO_2/NaCl(001), we can compare our results to those obtained by Liu *et al.* in another HAS diffraction study.[17] In the latter study the NaCl sample was exposed to an effusive CO_2 beam while the sample temperature was lowered. As in our case, coverage was monitored by following the intensity of the specular beam during exposure. The (2×1) structure proposed by Liu *et al.* for their low-coverage phase, i.e. 30% of a monolayer, reflects the (2×1) adsorbate lattice of CO_2 molecules adsorbed in large islands. The existence of a glide plane, which manifests itself only through missing diffraction peaks in the $\langle110\rangle$ direction (azimuthal angle 0°), was excluded in their analysis because of the appearance of a single diffraction feature which was attributed to the $(-1,0)$ peak [$(\frac{1}{2},0)$ in our nomenclature]. However, this feature is most prominent for an azimuthal angle of 20° and was not detectable in their work at 0°, the only angle where it should have been observed. We therefore exclude that it is due to the $(-1,0)$ superstructure peak, and conclude that the observed (2×1) unit mesh contains glide planes, according to the interpretation presented here. At $T_s=74$ K Liu *et al.* observed the growth of a second layer. While for the preparation of the submonolayer the effusive CO_2 beam was stopped at 92 K, well above second-layer formation, their high-coverage monolayer phase was established by lowering the sample temperature under continuous gas flow to 73 K, where the gas flow was stopped, then raising it to 76 K, and lowering it to 37 K where the scattering experiments were performed. To explain the measured diffraction pattern a $(2\sqrt{2}\times2\sqrt{2})R45°$ unit cell with 8 CO_2 molecules was proposed. We believe that the assumption of a $p(2\times2)$ instead of the $(2\sqrt{2}\times2\sqrt{2})R45°$ structure is sufficient to explain all data points not in agreement with a (2×1) structure (Fig. 5 in Ref. 17). The $p(2\times2)$ structure corresponds to a superposition of the (2×1) monolayer and the $c(2\times2)$ multilayer symmetry for the case of exposures of less than 170 L of CO_2. We therefore suggest that the high-coverage monolayer phase prepared by Liu *et al.* may have been a monolayer adsorbate partially covered with multilayers, e.g., due to additional CO_2 condensation during cooling to 37 K or due to incomplete multilayer desorption while rising the temperature from 73 to 76 K.

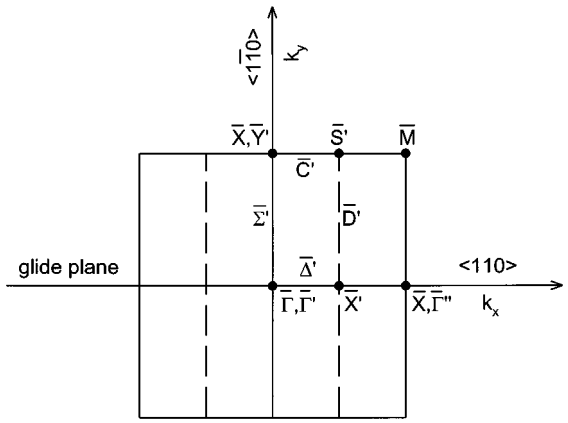

FIG. 9. Surface Brillouin zone of NaCl(001) (solid lines) and the Brillouin zone of the CO_2 monolayer superstructure (dashed line). The $\langle110\rangle$ and $\langle\bar{1}10\rangle$ directions correspond to the NaCl structure. Symbols corresponding to the superstructure Brillouin zone are marked by $'$.

Prior to an interpretation of the normal mode vibrations of the CO_2 molecules adsorbed on the NaCl surface some symmetry considerations are appropriate. Due to the (2×1) superstructure of the CO_2 monolayer the Brillouin zone of the adsorbate is different from the surface Brillouin zone of the NaCl(001) substrate as shown in Fig. 9. The characteristic points Γ, Γ', and Γ'' correspond to phonon wave vectors at the origin $Q=0$, while those labeled X, X', and Y' correspond to $Q=\pi/a$, with a being the lattice constant in the respective direction. All symbols marked by a prime refer to the adsorbate lattice. Two types of adlayer domains exist, one with the glide plane along the $\langle110\rangle$ direction of the NaCl(001) surface and one which is rotated by 90° with the glide plane along the $\langle\bar{1}10\rangle$ direction. Because both types of domains are always present TOF spectra measured for a given direction are in fact a superposition of both domains.

The phonon modes can be classified according to the symmetry group of their wave vector.[47] In the Δ' direction,

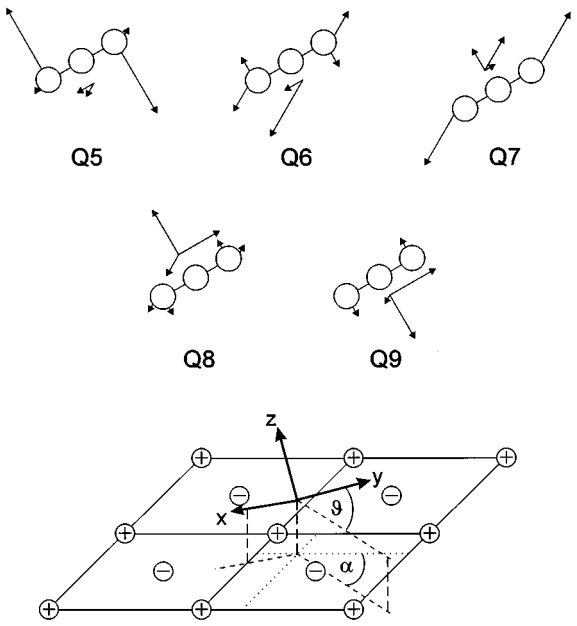

FIG. 10. Calculated ''external'' normal modes of monolayer CO_2 adsorbed on NaCl(001) (adapted from Refs. 20,21). Arrows directly attached to the molecule indicate rotational motions, others translation of the whole molecule. The CO_2 is adsorbed between Na^+ and Cl^-, with a tilt angle $\vartheta=26°$ relative to the surface plane and an azimuthal angle $\alpha=43°$ between the projection of the molecular axis onto the surface and a Na^+–Na^+ row.

along the longer side of the unit cell, there are two classes of modes with either even or odd displacement patterns with respect to the glide plane. The same applies for the $\bar{\Gamma}'$, $\bar{X}'$, and $\bar{Y}'$ points whereas in the $\bar{\Sigma}'$ direction no such symmetry exists. With two molecules per unit cell each of the five external modes of a single adsorbed CO_2 molecule splits into two and therefore altogether ten external phonon modes are expected for the $\bar{\Delta}'$ as well as for the $\bar{\Sigma}'$ direction. This ''Davydov'' splitting can be described on the basis of the exciton model.[48] However, for the $\bar{\Delta}'$ direction selection rules apply. (i) The split modes are of even and odd symmetry, respectively, and are necessarily degenerate at $\bar{X}'$.[49] (ii) The symmetry of the transition under consideration allows us to observe even modes in even (first, third, ...) and odd modes in odd (second, fourth, ...) Brillouin zones only.[50,51] Due to the superposition of $\bar{\Delta}'$ and $\bar{\Sigma}'$ which are measured simultaneously in our experiment the maximum number of modes observable for a given ΔK is therefore 15. In our presentation of the data all phonon wave vectors Q are folded into the first Brillouin zone, thus rendering possible detection of all 20 modes. However, not all these modes must be split in energy, and the interaction of the helium atoms is largest for modes with large displacement perpendicular to the surface. Therefore not all of them may be detected.

From a model adsorption potential of the monolayer CO_2 on NaCl(001) Heidberg and co-workers were able to deduce the normal modes of the adsorbed molecules.[20,21] Their potential which produced both the adsorption energy and the molecular orientation in good agreement with the FTIR data appears to be quite reliable. As expected for a linear molecule, their analysis yields for each adsorbed CO_2 four ''internal'' and five ''external'' normal modes, the latter of which are sketched in Fig. 10 (the ''internal'' modes are the symmetric stretch ν_1, the twofold degenerate bending vibration ν_2, and the asymmetric stretch ν_3, while the ''external'' modes are vibrational motions of the molecule against the surface). Only the in-phase vibration of all modes at $\bar{\Gamma}$ was calculated. The ''external'' modes were found to have energies between 17.4 and 71.4 cm^{-1} corresponding to between 2.2 and 8.9 meV, respectively.[52] Due to the use of the second derivative of the adsorption potential for the calculation of the normal mode frequencies the absolute values are to be interpreted with some caution. However, the relative sequence in energy is expected to be correct. All calculated external motions have components perpendicular to the surface. Therefore, since HAS is especially sensitive to such motions, it should be possible to observe all of them in these experiments, but due to different perpendicular amplitudes of the five modes different TOF peak intensities are expected.

In the present study the optical phonon modes IIIa and V were clearly visible at the zone origin $\bar{\Gamma}$ for both experimental incident wave vectors, their energies being 6.0 and 7.5 meV, corresponding to 48 and 60 cm^{-1}, respectively (see Fig. 8). Two more modes, I and IIa, have frequencies of about 3.6 meV (29 cm^{-1}) at $\bar{\Gamma}$ but are not unambiguously observable in the experiments with lower beam energy. As pointed out in Sec. III, this may be due to a strong coupling to the substrate and a damping of their amplitudes. For the smaller k_i some points are also observable at 9.2 meV (74 cm^{-1}), close to $\bar{\Gamma}$ and $\bar{\Gamma}''$ ($\bar{Y}'$). The errors were estimated to be ± 0.25 meV$\equiv 2$ cm^{-1} for all these modes. Features at higher energy losses in the measurements with the incident beam energy $E_i=33.5$ meV ($k_i=8.02$ $Å^{-1}$) can be most probably assigned to excitation of overtones or combination bands. Indications for this are provided by the relative intensities of the observed energy loss features as well as results from mixed rare gas layers. (i) In our experiments with higher incident beam energy of 33.5 meV the most intense mode is that at about 7.5 meV, followed by the feature corresponding to the modes around 3.6 meV which are not resolved in these measurements. The other three features at 11.0, 14.8, and 18.5 meV are very weak in comparison. (ii) For a perfectly mixed Ar/Kr(1/1) adlayer on Pt(111) Kern *et al.* observed no ''mixed'' (Ar+Kr) energy losses, although the overtones of the Einstein modes of both rare gases were apparent.[53] This result strongly suggests that also in our experiments the excitations observed at 11, 14.8, and 18.5 meV are due to local interaction of a helium atom with one single CO_2 molecule, i.e., the energy transfer occurs in a single scattering event and not in two or three steps. Although barely visible, the energy losses found at 11 and 18.5 meV would be the first evidence for the observation of combination modes by HAS so far. The polarization of these modes is expected to be the same as for the corresponding fundamentals.

Table I summarizes the measured energy loss and gain features and their tentative assignment to the normal modes calculated by Heidberg *et al.*[20,21] To all expected modes we can assign a measured phonon mode. As mentioned above

TABLE I. Assignment of measured to calculated (Refs. 20 and 21) normal mode energies. Relative intensity scale: (s) strong, (m) medium strong, (w) weak. The bracketed numbers behind the calculated energies give the order of (calculated) mode components perpendicular to the surface.

Normal mode	Calculated energy (meV) and intensity	Measured energy (meV)
Q_5	2.2 (3)	two modes at 2–4 meV
Q_6	3.2 (5)	(m–s)
Q_7	4.1 (2)	6.0 (m–s)
Q_8	6.8 (1)	7.5 (s)
Q_9	8.9 (4)	9.2 (m–s)

the helium atoms are expected to interact most strongly with motions of the CO_2 molecules with large amplitude perpendicular to the surface. From the calculated normal modes it can be deduced that the normal modes Q_8 and Q_7 have the largest relative amplitudes perpendicular to the surface, followed by Q_5, Q_9, and Q_6.[20,21,54] We tentatively attribute the Q_5 mode, with a calculated energy of 2.2 meV, to the lower loss in the 2–4 meV range, the Q_8 mode with a calculated energy of 6.8 meV to the 7.5 meV feature, and Q_7 (4.1 meV) to the 6 meV feature. According to the calculation Q_5 can best be visualized as a ''frustrated rotation'' while Q_7 and Q_8 have predominantly the character of z-polarized modes. The other calculated modes Q_6 and Q_9 have weaker relative amplitudes perpendicular to the surface. We assign them to the measured modes according to their increasing energy; the higher loss in the 2–4 meV range is attributed to Q_6, the 9.2 meV phonon to Q_9.

It is interesting to note that the width of some energy loss and gain features, e.g., mode V, is apparently larger than the instrumental resolution. This increase in width may be an indication for a nonresolved splitting of some of the normal modes into two modes. As discussed above the Davydov splitting is expected due to the correlation field between the two CO_2 molecules in the (2×1) unit cell. It was detected in infrared spectroscopy for the asymmetric stretching vibration ν_3 as well as for the twofold degenerate bending vibration ν_2. This splitting, which is about 1.1 meV (9 cm^{-1}) in the case of ν_3, depends linearly on the vibrational polarizability α_v and on the frequency.[7,55] The α_v of an ''external'' mode is very small.[7] The correlation field splitting and dispersion due to dipole–dipole coupling of the external modes is expected to be much less than 1 meV,[56] and probably cannot be unambiguously resolved by present HAS machines. The strong dispersion of the modes IIb and IIIb can therefore not be explained by dipole–dipole coupling. It suggests that modes with a large in-plane amplitude probably have been detected in our experiments, and that the dispersion is due to short-range interactions which are more important than for the internal vibrations. The splitting of these modes can be estimated from this observed dispersion to be in the meV range.

In a very recent study Picaud, Hoang, and Girardet tried to interpret the dispersion curves for the CO_2 monolayer adsorbed on NaCl(001) (Ref. 26) on the basis of a semiempirical potential.[25] The various observed branches are identified in terms of coupled translational and librational modes by solving the dynamical matrix of the adsorbate lattice unit cell, for two perpendicularly oriented domains. Comparable to the less complex normal coordinate analysis,[20,21] it is found that the hybridization of different motions is significant, due to a large influence of lateral interactions. Altogether 20 modes were predicted with energies at $\bar{\Gamma}$ ranging from 1.5 to 13.3 meV, with eight modes lying above 10 meV, somewhat higher than probably observed in our experiment. Due to the lateral coupling between the motions of the two molecules in the adsorbate lattice unit cell, five pairs of two branches are observed which are split by 0.4–1.4 meV at $\bar{\Gamma}$. In addition, each of these branches splits into two by up to 1 meV in the two different domain orientations. All of these modes have components perpendicular to the surface and should be accessible to HAS.

To our knowledge, the recent theoretical study by Picaud, Hoang, and Girardet is the as yet most complete calculation of the dynamics of a complex adsorbate system. Although the agreement between experiment and theory is not yet perfect, important conclusions on the interpretation of the experimental data are possible. (i) All five ''external'' vibrations which already result from the simpler normal coordinate treatment are split into a doublet. Although this splitting is probably unresolved, it possibly explains the observed phonon broadening. (ii) The two different domain orientations cause an additional splitting by two for each of the ten branches (except at the zone origin), thus rendering possible detection of up to twenty phonon modes as concluded from the symmetry arguments presented above.

Unfortunately in this theoretical investigation the coupling of the adsorbate vibration with the substrate phonons was not included. As discussed in connection with Fig. 8 the hybridization has an important effect on the intensities and also on the frequencies of the adsorbate modes. A more detailed theoretical study with consideration of the dynamical coupling with the substrate would be highly desirable. Also a more detailed HAS experiment is called for where special attention should be given to extracting the relative intensities of the various inelastic peaks. In this way it should ultimately be possible to assign the many observed modes. Then with future best-fit calculations it should be possible to pin down the adsorbate–adsorbate and adsorbate–substrate interaction coupling constants quite precisely.

V. CONCLUSIONS

The monolayer and multilayers of carbon dioxide physisorbed on sodium chloride single crystal surfaces cleaved *in situ* under ultrahigh vacuum were studied by means of helium atom scattering. The monolayer adsorbate structure was characterized by diffraction under adsorption–desorption equilibrium conditions, at $p(CO_2)=1\times10^{-9}$–1×10^{-8} mbar and $T_s=80-83.5$ K. The diffraction patterns for different azimuths uniquely identify the adsorbate structure as a (2×1) lattice commensurate to the substrate and with a glide plane. The unit cell belongs to the two-dimensional space group pg. This result is in agreement with data from LEED (Ref. 16) and FTIR spectroscopy[2,3,5–8,10,11,20,21] but disagrees with a previous HAS study.[17] In the helium atom time-of-flight spectra from the monolayer a large number of sharp low-energy loss and gain features could be resolved, which are

not present on the bare NaCl(001) surface. Many of the peaks can be attributed to single phonon excitation of external normal modes, corresponding to vibrations of the adsorbed molecules with respect to the surface. Based on a comparison with calculated normal modes[20,21] we tentatively attribute the stronger features to a ''frustrated rotation'' (2–4 meV) and to ''frustrated translations'' (6 and 7.5 meV, respectively). The interpretation of the experimental data are aided by a very recent lattice dynamical calculation.[26] Although barely visible, energy losses found at 11 and 18.5 meV are probably the first evidence for the observation of combination modes by HAS so far.

Upon condensation beyond a monolayer additional CO_2 grows commensurate on top of the full CO_2 monolayer. A superposition of the (2×1) monolayer symmetry and the $c(2\times2)$ symmetry of solid CO_2 was observed up to exposures of about 170 L. Possible explanations for this coexistence include (i) an unexpected low sticking coefficient, so that in fact only very few CO_2 layers are formed even after a dosage of 170 L; (ii) cluster (e.g., pyramidal) growth of the solid or (iii) unexpected structural changes in the first layers of solid CO_2 as compared to the infinite solid.

As a final remark we want to emphasize the unique position of helium atom scattering in the investigation of adsorption on alkali halide single crystal surfaces. Not only does helium atom diffraction provide the symmetry and structure of the adsorbate lattice but the time-of-flight spectra provide the low-energy (thermal) normal mode frequencies of adsorbed molecules on the surface. The thermal excitation of just these modes is the activating step in a number of important dynamical processes such as site conversion, diffusion, desorption, and vibrational line broadening mechanisms.

ACKNOWLEDGMENTS

We thank Dr. G. Brusdeylins, Dr. R. Kühnemuth, and Dr. O. Schönekäs for helpful discussions, Professor J. Heidberg for encouragement and support, and Professor L. Bruch for critically reading the manuscript. H. W. would like to thank the Fonds der Chemischen Industrie for a Liebig-Stipendium and the DFG for a Habilitandenstipendium.

[1] H.-C. Chang, and G. E. Ewing, J. Phys. Chem. **94**, 7635 (1990); R. Disselkamp, H.-C. Chang, and G. E. Ewing, Surf. Sci. **240**, 193 (1990); D. Dai and G. E. Ewing, J. Electron Spectrosc. Relat. Phenom. **64/65**, 101 (1993), and references therein.
[2] J. Heidberg, E. Kampshoff, and M. Suhren, J. Chem. Phys. **95**, 9408 (1991).
[3] J. Heidberg, E. Kampshoff, R. Kühnemuth, O. Schönekäs, and M. Suhren, J. Electron Spectrosc. Relat. Phenom. **54/55**, 945 (1990).
[4] J. Heidberg, M. Suhren, and H. Weiss, Ber. Bunsenges. Phys. Chem. **95**, 1680 (1991); J. Heidberg, M. Suhren, and H. Weiss, J. Electron Spectrosc. Relat. Phenom. **64/65**, 227 (1993), and references therein.
[5] J. Heidberg, E. Kampshoff, O. Schönekäs, H. Stein, and H. Weiss, Ber. Bunsenges. Phys. Chem. **94**, 118 (1990); J. Heidberg, E. Kampshoff, R. Kühnemuth, O. Schönekäs, H. Stein, and H. Weiss, Surf. Sci. **226**, L43 (1990).
[6] J. Heidberg, E. Kampshoff, R. Kühnemuth, and O. Schönekäs, Surf. Sci. **269/270**, 120 (1992).
[7] J. Heidberg, E. Kampshoff, R. Kühnemuth, O. Schönekäs, G. Lange, D. Schmicker, J. P. Toennies, R. Vollmer, and H. Weiss, J. Electron Spectrosc. Relat. Phenom. **64/65**, 341 (1993).
[8] J. Heidberg, E. Kampshoff, R. Kühnemuth, and O. Schönekäs, J. Electron Spectrosc. Relat. Phenom. **64/65**, 803 (1993).
[9] J. Heidberg and W. Häser, J. Electron Spectrosc. Relat. Phenom. **54/55**, 971 (1990).
[10] O. Berg and G. E. Ewing, Surf. Sci. **220**, 207 (1989).
[11] O. Berg, R. Disselkamp, and G. E. Ewing, Surf. Sci. **277**, 8 (1992).
[12] O. Berg, L. Quattrocci, S. K. Dunn, and G. E. Ewing, J. Electron Spectrosc. Relat. Phenom. **54/55**, 981 (1990).
[13] H.-C. Chang and G. E. Ewing, Phys. Rev. Lett. **65**, 2125 (1990).
[14] D. Schmicker, J. P. Toennies, R. Vollmer, and H. Weiss, J. Chem. Phys. **95**, 9412 (1991).
[15] G. Lange, J. P. Toennies, R. Vollmer, and H. Weiss, J. Chem. Phys. **98**, 10 096 (1993).
[16] J. Schimmelpfennig, S. Fölsch, and M. Henzler, Surf. Sci. **250**, 198 (1991).
[17] G.-Y. Liu, G. N. Robinson, G. Scoles, and P. A. Heiney, Surf. Sci. **262**, 409 (1992).
[18] P. M. Blass, R. C. Jackson, J. C. Polanyi, and H. Weiss, J. Electron Spectrosc. Relat. Phenom. **54/55**, 993 (1990); J. Chem. Phys. **94**, 7003 (1991).
[19] See, e.g., J. E. Lennard-Jones and B. M. Dent, Trans. Faraday Soc. **24**, 92 (1928); R. Gevirzman, Y. Kozirovski, and M. Folman, *ibid*. **65**, 2206 (1969); J. Heidberg, R. D. Singh, and C. F. Chen, Z. Phys. Chem. N. F. **110**, 135 (1978); J. C. Polanyi, R. J. Williams, and S. F. O'Shea, J. Chem. Phys. **94**, 978 (1991).
[20] J. Heidberg, E. Kampshoff, R. Kühnemuth, and O. Schönekäs, Surf. Sci. **251/252**, 314 (1991).
[21] A refinement of the potential presented in Ref. 20 resulted in the following structural parameters: heat of adsorption=32.5 kJ mol^{-1} (monolayer), 28 kJ mol^{-1} (submonolayer); tilt angle relative to the surface=28°; azimuthal angle enclosed by two molecules=86°; frequencies of the external vibrations $Q_5=17.4$ cm^{-1}, $Q_6=25.9$ cm^{-1}, $Q_7=32.7$ cm^{-1}, $Q_8=54.5$ cm^{-1}, $Q_9=71.4$ cm^{-1} [O. Schönekäs (unpublished)].
[22] J. C. Polanyi, R. J. Williams, and S. F. O'Shea, J. Chem. Phys. **94**, 978 (1991).
[23] G. P. M. Poppe, C. M. J. Wijers, and A. van Silfhout, Surf. Sci. **251/252**, 321 (1991).
[24] W. Chen and W. L. Schaich, Surf. Sci. **218**, 580 (1989); **220**, L733 (1989).
[25] C. Girardet, S. Picaud, and P. N. M. Hoang, Europhys. Lett. **25**, 131 (1994).
[26] S. Picaud, P. N. M. Hoang, and C. Girardet, Surf. Sci. **322**, 381 (1995).
[27] V. Celli, D. Eichenauer, A. Kaufhold, and J. P. Toennies, J. Chem. Phys. **83**, 2504 (1985).
[28] G. Brusdeylins, R. B. Doak, and J. P. Toennies, Phys. Rev. B **27**, 3662 (1983).
[29] J. P. Toennies and R. Vollmer, Phys. Rev. B **44**, 9833 (1991).
[30] Dr. Karl Korth Monokristalle-Kristalloptik oHG, Am Jägersberg 3, D-24161 Altenholz (Kiel).
[31] G. Benedek, G. Brusdeylins, R. B. Doak, J. G. Skofronick, and J. P. Toennies, Phys. Rev. B **28**, 2104 (1983).
[32] G. Lilienkamp and J. P. Toennies, J. Chem. Phys. **78**, 5210 (1983).
[33] J. P. Toennies and R. Vollmer, Phys. Rev. B **40**, 3495 (1989).
[34] The transfer width of 450 Å was estimated from the width of diffraction spots measured for bare NaCl(001). In the calculation a perfect, infinitely extended single crystal surface was assumed. This assumption is supported by own atomic force microscopy measurements which show smooth extended terraces having a width of several 100 nm.
[35] B. W. Holland and D. P. Woodruff, Surf. Sci. **36**, 488 (1973).
[36] *International Tables for X-ray Crystallography*, edited by N. F. M. Henry and K. Lonsdale (Kynoch, Birmingham, 1952), Vol. 1.
[37] S. A. Safron, W. P. Brug, G. G. Bishop, G. Chern, M. E. Derrick, J. Duan, M. E. Deweese, and J. G. Skofronick, J. Vac. Sci. Technol. A **9**, 1657 (1991).
[38] K. Kern, P. Zeppenfeld, R. David, and G. Comsa, Phys. Rev. B **35**, 886 (1987).
[39] Th. Wach, Diploma thesis, Göttingen, 1991.
[40] B. Redlich and H. Weiss (unpublished).
[41] B. Poelsema, G. Mechtersheimer, and G. Comsa, Phys. Rev. Lett. **49**, 578 (1982).
[42] J. P. Toennies, in *Surface Phonons*, edited by W. Kress and F. W. de Wette (Springer, Berlin, 1991), pp. 111–166.
[43] J. J. deMiguel, A. Sànchez, A. Cebollada, J. M. Gallego, J. Ferròn, and S. Ferrer, Surf. Sci. **189/190**, 1062 (1987).
[44] D. Schmicker, J. P. Toennies, R. Vollmer, and H. Weiss (unpublished).

[45] R. C. Wyckoff, *Crystal Structures*, 2nd ed. (Interscience, New York, 1965), Vol. 1.
[46] C. Argile and G. E. Rhead, Surf. Sci. Rep. **10**, 277 (1989).
[47] A. P. Cracknell, Thin Solid Films **21**, 107 (1974).
[48] A. S. Davydov, *Theory of Molecular Excitons* (McGraw–Hill, New York, 1962).
[49] F. Hund, Z. Phys. **99**, 119 (1936).
[50] B. Voigtländer, D. Bruchmann, S. Lehwald, and H. Ibach, Surf. Sci. **225**, 151 (1990).
[51] K. C. Prince, J. Electron Spectrosc. Relat. Phenom. **42**, 217 (1987).
[52] From a fit of a dephasing model to the vibrational frequency and linewidth data the same authors could deduce another value for an external motion, 41–50 cm^{-1} (corresponding to 5.1–6.3 meV). See Ref. 3.
[53] K. Kern, P. Zeppenfeld, R. David, and G. Comsa, J. Electron Spectrosc. Relat. Phenom. **44**, 215 (1987).
[54] O. Schönekäs (private communication). In the calculations the amplitude was normalized to 1 for each mode.
[55] H. Weiss, Surf. Sci. (in press).
[56] G. D. Mahan and A. A. Lucas, J. Chem. Phys. **68**, 1344 (1978).